# Synthesis, spectroscopy, and structures of the seven-coordinate complexes $(CH_3)_2AsC(CF_3){=}C(CF_3)As(CH_3)_2W(CO)_2I_2P(OC_6H_5)_3$ and $[(CH_3)_2AsC(CF_3){=}C(CF_3)As(CH_3)_2]_2W(CO)Br_2$ and spectroscopy of related seven-coordinate complexes

**Richard J. Barton, Sushil K. Manocha, Beverly E. Robertson, and Lynn M. Mihichuk**

**Abstract**: (L-L)W(CO)$_3$I$_2$ (L-L = $(CH_3)_2AsC(CF_3){=}C(CF_3)As(CH_3)_2$) reacts with the monodentate phosphite $P(OC_6H_5)_3$ and (L-L)W(CO)$_3$Br$_2$ reacts with L-L to form new seven-coordinate complexes (L-L)W(CO)$_2$I$_2$P(OC$_6$H$_5$)$_3$ and (L-L)$_2$W(CO)Br$_2$. Low-temperature X-ray diffraction analyses show the tungsten atom to be seven coordinate in both complexes, with the geometry most closely approximated by a monocapped octahedral environment, the capping group being a carbonyl in the dicarbonyl complex; the geometry is most closely approximated by a pentagonal bipyramidal environment in the monocarbonyl complex. The $^1$H, $^{13}$C, and $^{19}$F NMR data indicate that the dicarbonyl complex is stereochemically nonrigid at 298 K and rigid at lower temperatures, while the monocarbonyl is nonrigid both at 298 K and at lower temperatures. $\Delta G^{\neq}$ values calculated at coalescence temperatures are consistent with an intramolecular rearrangement process for both complexes. The $^{13}$C chemical shifts and $^2J(^{13}C\text{-}^{31}P)$ values provide important structural considerations in the assignment of a seven-coordinate geometry. Spectroscopic properties for the related seven-coordinate dicarbonyl complexes (L-L)W(CO)$_2$PX$_2$ (P = P(OC$_6$H$_5$)$_3$; X = Br; P = P(OCH$_3$)$_3$, P(C$_6$H$_5$)$_3$; X = Br, I) and monocarbonyl complexes (L-L)$_2$W(CO)I$_2$ and (L-L)W(CO)X$_2$[P(OCH$_3$)$_3$]$_2$ (X = Br, I) are presented and compared to those of the two title complexes.

*Key words*: seven-coordination, X-ray, NMR analysis.

**Résumé** : Le (L-L)W(CO)$_3$I$_2$ (L-L = $(CH_3)_2AsC(CF_3){=}C(CF_3)As(CH_3)_2$) réagit avec le phosphite monodentate $P(OC_6H_5)_3$ alors que (L-L)W(CO$_3$)Br$_2$ réagit avec L-L pour former respectivement les nouveaux complexes heptacoordinés (L-L)W(CO)$_2$I$_2$P(OC$_6$H$_5$)$_3$ et (L-L)$_2$W(CO)Br$_2$. Des analyses de diffraction des rayons X à basse température ont permis de montrer que l'atome de tungstène est heptacoordiné dans les deux complexes: dans le complexe dicarbonyle, sa géométrie peut être décrite approximativement par un environnement octaédrique à cap unique qui est le dicarbonyle; dans le complexe monocarbonyle, la géométrie peut être décrite approximativement par un environnement bipyramidal pentagonal. Les données de RMN du $^1$H, du $^{13}$C et du $^{19}$F indiquent que le complexe dicarbonyle est stéréochimiquement non rigide à 298 K mais qu'il est rigide à des températures inférieures; par ailleurs, le complexe monocarbonyle n'est pas rigide ni à 298 K ni à des températures inférieures. Pour chacun de ces complexes, les valeurs de $\Delta G^{\neq}$ calculées à partir des températures de coalescence sont en accord avec un processus de réarrangement intramoléculaire. Les valeurs des déplacements chimiques en $^{13}$C ainsi que celles des $^2J(^{13}C\text{-}^{31}P)$ fournissent des considérations structurales importantes dans l'attribution de la géométrie heptacoordinée. On rapporte les propriétés spectroscopiques des complexes dicarbonyles heptacoordinés apparentés (L-L)W(CO)$_2$PX$_2$ (P = P(OC$_6$H$_5$)$_3$; X = Br; P = P(OCH$_3$)$_3$ ou P(C$_6$H$_5$)$_3$; X = Br, I) et des complexes monocarbonyles (L-L)$_2$W(CO)I$_2$ et (L-L)W(CO)X$_2$[P(OCH$_3$)$_3$]$_2$ (X = Br, I) et on les compare à celles des deux complexes mentionnés dans le titre.

*Mots clés* : heptacoordination, rayons X, analyse par RMN.

[Traduit par la rédaction]

## Introduction

In the area of seven coordination the relevant polytopal polyhedra are the pentagonal bipyramid, the monocapped octahedron, and the quadrilaterally monocapped trigonal prism. X-ray crystallographic studies of seven-coordinate transition metal carbonyl complexes have shown the latter two types of geometry to predominate (1–12). However, the actual structures seldom match the ideal polyhedral arrangements, and

Received August 12, 1997.

**R.J. Barton, S.K. Manocha, B.E. Robertson, and L.M. Mihichuk.**[1] Department of Chemistry, University of Regina, Regina, SK S4S 0A2, Canada.

[1] Author to whom correspondence may be addressed. Telephone: (306) 585-4793. Fax: (306) 585-4894. E-mail: mihichuk@meena.cc.uregina.ca

Can. J. Chem. **76**: 245–253 (1998)

various criteria have been proposed to aid in the assignment of the most appropriate description to an experimentally determined polyhedron (13–15).

We have been interested in the seven-coordinate chemistry of group six metal (Mo, W) carbonyl complexes from the point of view of structure and dynamic behaviour (10–12, 16). Structural studies have been restricted to the tungsten analogues because the corresponding molybdenum complexes decompose in the X-ray beam during X-ray analysis, preventing the collection of useful structural data. In addition the 14.4% spin one-half $^{183}$W atom provides important coupling parameters not present in the molybdenum series. The molybdenum and tungsten complexes nevertheless show similar properties and are assumed to behave in a similar manner with regard to fluxionality and reactivity. Our present study, which includes a detailed spectroscopic investigation of tungsten complexes containing one bidentate ligand and extends into a study of corresponding complexes incorporating two bidentate ligands, allows for a greater understanding of structural features in terms of a predominant geometry and fluxional behaviour.

Seven-coordinate carbonyl complexes also exhibit fluxionality in solution, resulting in room-temperature NMR spectra often not being consistent with the X-ray crystal structure. The reason for this behaviour is thought to be due to the small energy barriers between stereochemical isomers. To explain the mechanisms of these dynamic processes both intramolecular and (or) intermolecular pathways are possible (14, 16–18), and no typical mechanism is responsible for these processes although most are described as intramolecular rearrangements. We are compiling structural and solution NMR data in order to better understand the dynamic behaviour and elucidate the mechanism of the ligand motion.

In this paper we describe the synthesis, X-ray structure, spectroscopic properties, and fluxional behaviour of the seven-coordinate complexes $(CH_3)_2AsC(CF_3){=}C(CF_3)As(CH_3)_2$-$W(CO)_2I_2P(OC_6H_5)_3$ and $[(CH_3)_2AsC(CF_3){=}C(CF_3)As(CH_3)_2]_2$-$W(CO)Br_2$ and spectroscopic properties of related seven-coordinate complexes.

## Experimental section

### General considerations

All reactions were carried out under an argon atmosphere using standard Schlenk tube techniques. Solvents were dried and purified by known procedures and distilled under nitrogen prior to use. The ligand *cis*-2,3-bis(dimethylarsino)-1,1,1,4,4,4-hexafluorobut-2-ene(L-L) (19, 20) and the starting complexes (L-L)$W(CO)_3I_2$ and (L-L)$W(CO)_3Br_2$ were prepared as previously described (16).

All seven-coordinate dicarbonyl complexes for which spectroscopic data are presented were prepared in a similar manner to that of (L-L)$W(CO)_2I_2P(OC_6H_5)_3$, discussed below. Specifically, the preparation of (L-L)$W(CO)_2I_2P(OCH_3)_3$ (11) and (L-L)$W(CO)_2Br_2P(C_6H_5)_3$ (12) have been previously described. The synthesis of the seven-coordinate monocarbonyl complex (L-L)$W(CO)Br_2[P(OCH_3)_3]_2$ has been previously described (10), and the iodo analogue was prepared in a similar manner to that of $(L\text{-}L)_2W(CO)Br_2$, discussed below, as was $(L\text{-}L)_2W(CO)I_2$.

**Table 1.** Crystallographic data for (L-L)$W(CO)_2I_2P(OC_6H_5)_3$ and $(L\text{-}L)_2W(CO)Br_2$.

| | **(L-L)$W(CO)_2I_2P(OC_6H_5)_3$** | **$(L\text{-}L)_2W(CO)Br_2$** |
|---|---|---|
| Mol. formula | $C_{28}H_{27}As_2F_6I_2O_5PW$ | $C_{17}H_{24}As_4Br_2F_{12}OW$ |
| Mol. wt. | 1175.91 | 1115.58 |
| Cryst. syst. | Monoclinic | Monoclinic |
| Space group | $C2/c$ | $P2_1/c$ |
| $a$, Å | 24.444(2) | 14.073(2) |
| $b$, Å | 15.704(1) | 14.523(2) |
| $c$, Å | 19.038(1) | 29.434(4) |
| β, deg | 97.12(1) | 105.08(2) |
| $V$, Å$^3$ | 7252 | 5808 |
| $Z$ | 8 | 8 |
| $D_{calcd}$, g cm$^{-3}$ | 2.15 | 2.55 |
| $D_{measd}$, g cm$^{-3}$ | 2.20 | 2.48 |
| $F(0,0,0)$ | 4400 | 4144 |
| μ(Mo Kα), cm$^{-1}$ | 69.06 | 120.25 |
| $R^a$ | 0.047 | 0.073 |
| $wR^b$ | 0.063 | 0.100 |

[a] $R = \Sigma||F_o| - |F_c||/\Sigma|F_o|$.

[b] $wR = [\Sigma w(|F_o| - |F_c|)^2/\Sigma w|F_o|^2]^{1/2}$.

The $^1$H, $^{31}$P-{$^1$H}, $^{19}$F-{$^1$H}, and $^{13}$C NMR data were recorded on a Bruker AC 200 QNP NMR spectrometer ($^1$H, 200.13 MHz; $^{31}$P, 81.02 MHz; $^{19}$F, 188.31 MHz; $^{13}$C, 50.3 MHz). Chemical shifts are expressed in parts per million, downfield from $Si(CH_3)_4$ ($^1$H, $^{13}$C), downfield (positive) or upfield (negative) from 85% $H_3PO_4$($^{31}$P) and upfield (negative) from $CFCl_3$($^{19}$F).

Infrared spectra were recorded on a Perkin–Elmer 1600 FT instrument in dichloromethane and are reported in cm$^{-1}$. Elemental analyses were measured using a Perkin–Elmer 2400 CHN elemental analyzer.

### Preparation of (L-L)$W(CO)_2I_2P(OC_6H_5)_3$

The (L-L)$W(CO)_3I_2$ (0.25 g, 0.28 mmol) and $P(OC_6H_5)_3$ (0.12 g, 0.32 mmol) were refluxed in 50 mL of benzene for 17 h. The infrared spectra indicated complete conversion of the tricarbonyl complex to the dicarbonyl complex. The solvent was removed in vacuo, and the resulting yellow solid was washed with *n*-hexane to remove any unreacted $P(OC_6H_5)_3$ and was then recrystallized from a dichloromethane hexane mixture at –20°C to give 0.25 g (75%) of (L-L)$W(CO)_2I_2P(OC_6H_5)_3$. $^1$H NMR ($CDCl_3$): 2.01 (s, 12H, $As(CH_3)_2$), 7.27 (m, 15H, $P(OC_6H_5)_3$); $^{31}$P-{$^1$H}NMR ($CDCl_3$): 90.7 (s, W-P, $J$($^{183}$W-$^{31}$P) = 403 Hz); $^{19}$F-{$^1$H}NMR ($CDCl_3$): –53.1 (s, $CF_3$). Anal. calcd. for $C_{28}H_{27}As_2F_6I_2O_5PW$: C 28.57, H 2.30, I 21.60; found: C 28.90, H 2.29, I 21.77.

### Preparation of $(L\text{-}L)_2W(CO)Br_2$

The (L-L)$W(CO)_3Br_2$ (0.25 g, 0.31 mmol) and (L-L) (0.25 g, 0.67 mmol) were refluxed in 50 mL of toluene for 22 h. The colour of the reaction mixture changed from yellow to orange to dark brown. Infrared spectroscopy indicated complete conversion of the tricarbonyl complex to the monocarbonyl complex. The solvent was removed in vacuo, and the resulting brown–black solid was recrystallized from a toluene–hexane mixture at –20°C to give 0.23 g (65%) of $(L\text{-}L)_2W(CO)Br_2$. $^1$H NMR ($CD_2Cl_2$): 2.05 (s, $As(CH_3)_2$); $^{19}$F-{$^1$H}NMR ($CDCl_3$): –50.6 (s, $CF_3$). Anal. calcd. for $C_{17}H_{24}As_4Br_2F_{12}OW$: C 18.29, H 2.15, Br 14.34; found: C 17.93, H 2.08, Br 14.81.

**Table 2.** Selected bond distances (Å) and angles (deg) for (L-L)W(CO)$_2$I$_2$P(OC$_6$H$_5$)$_3$.

| Bond | Distance (Å) | Bond | Distance (Å) |
|---|---|---|---|
| W—As(1) | 2.5603(7) | W—C(1) | 1.942(7) |
| W—As(2) | 2.6004(7) | W—C(2) | 1.957(8) |
| W—I(1) | 2.8684(6) | C(1)—O(1) | 1.16(1) |
| W—I(2) | 2.8698(7) | C(2)—O(2) | 1.17(1) |
| W—P | 2.457(2) | | |
| **Bond** | **Angle (deg)** | **Bond** | **Angle (deg)** |
| As(1)-W-As(2) | 76.02(2) | P-W-C(1) | 110.7(2) |
| As(1)-W-I(1) | 159.74(2) | P-W-C(2) | 77.2(2) |
| As(1)-W-I(2) | 76.88(4) | C(1)-W-C(2) | 71.2(3) |
| As(1)-W-P | 110.88(4) | W-C(1)-O(1) | 179.1(7) |
| As(1)-W-C(1) | 114.8(2) | W-C(2)-O(2) | 176.6(6) |
| As(1)-W-C(2) | 71.9(2) | W-As(1)-C(8) | 109.7(2) |
| As(2)-W-I(1) | 89.51(2) | W-As(1)-C(9) | 114.9(3) |
| As(2)-W-I(2) | 83.24(2) | W-As(1)-C(10) | 120.6(3) |
| As(2)-W-P | 161.67(4) | C(8)-As(1)-C(9) | 110.7(4) |
| As(2)-W-C(1) | 79.6(2) | C(8)-As(1)-C(10) | 98.9(3) |
| As(2)-W-C(2) | 121.0(2) | C(9)-As(1)-C(10) | 100.6(4) |
| I(1)-W-I(2) | 87.54(2) | W-As(2)-C(3) | 118.7(3) |
| I(1)-W-P | 79.09(4) | W-As(2)-C(4) | 115.4(3) |
| I(1)-W-C(1) | 75.4(2) | W-As(2)-C(5) | 110.3(2) |
| I(1)-W-C(2) | 128.2(2) | C(3)-As(2)-C(4) | 104.5(5) |
| I(2)-W-P | 82.00(4) | C(3)-As(2)-C(5) | 101.8(4) |
| I(2)-W-C(1) | 155.8(2) | C(4)-As(2)-C(5) | 104.3(4) |
| I(2)-W-C(2) | 132.7(2) | | |

**Fig. 1.** ORTEP diagram for (L-L)W(CO)$_2$I$_2$P(OC$_6$H$_5$)$_3$ showing the atomic labelling scheme with 50% probability thermal ellipsoids.

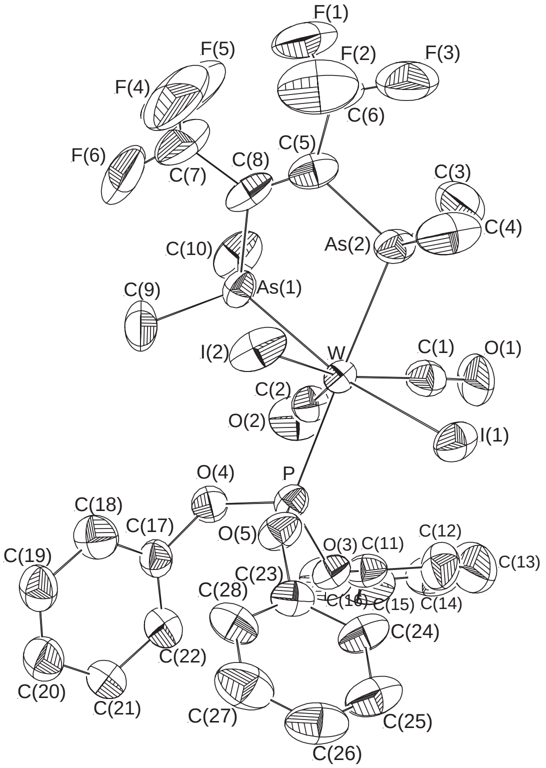

## Crystallographic characterization of (L-L)W(CO)$_2$I$_2$P(OC$_6$H$_5$)$_3$

A yellow–orange crystal with approximate dimensions 0.41 × 0.44 × 0.45 mm was selected and coated with collodion. Preliminary investigation of the precession photographs showed symmetry and systematic extinction conditions (*hkl*: $h + k = 2n$; *h*01: h, $l = 2n$; and 0*k*0: $k = 2n$) indicative of the space group *C*2/*c* or *Cc*. The accurate unit cell parameters were obtained from the least-squares refinement of 24 reflections and their Friedel pairs in the 2θ range 35–45°, as observed on a modified Picker FACS-1 four-circle diffractometer. The intensity data were collected at 218 ± 4 K using an Enraf–Nonius Universal low-temperature device. Three standard reflections were measured after every 47 reflections. No significant decay was observed during data collection.

The intensities of 8291 independent reflections were measured for 2θ values between 3° and 55° of which 6663 were considered to be observed with $I \geq 2\sigma(I)$. Absorption corrections were applied using the Gaussian integration method. The crystal data are given in Table 1. The intensity statistics indicated the centrosymmetric space group *C*2/*c*. The structure was solved by combined direct methods and Fourier syntheses. All non-hydrogen atoms were refined anisotropically by the full-matrix least-squares method. Weights were assigned according to the REGWT program with $w = (\sigma_c^2 + \sigma_m^2)^{-1}$, where $\sigma_c^2$ is the variance and $\sigma_m^2$ is the term calculated by REGWT using iterative methods to remove the systematic trends with respect to *F* and sin θ/λ in the residuals of the structure factors (21). Several cycles of least-squares refinement were performed to achieve a convergence with a conventional *R* value of 0.047 and a weighted *R* value of 0.063. The maximum and average shift/esd of the least-squares parameters were $1.8 \times 10^{-3}$ and $1.1 \times 10^{-4}$, respectively. In the final Fourier difference map a peak corresponding to 1.71 e Å$^{-3}$ was located approximately 1.07 Å from the center of the W atom. The residual density near the heavy transition metal is not unexpected in light of the approximations used in the absorption corrections. All calculations were carried out using the XTAL 2.4 system of programs (22). Important bond lengths and bond angles are given in Table 2.[2] An ORTEP drawing showing the atomic labelling scheme is given in Fig. 1, and a schematic diagram showing the torsional angles in the five-membered ring of the chelate ligand for (L-L)W(CO)$_2$I$_2$P(OC$_6$H$_5$)$_3$ and (L-L)W(CO)$_2$I$_2$P(OCH$_3$)$_3$ is given in Fig. 2.

## Crystallographic characterization of (L-L)$_2$W(CO)Br$_2$

Brown–black plates were crystallized from a toluene–hexane

---

[2] The supplementary material includes tables of atomic coordinates for the non-hydrogen atoms, additional bond distances and angles, anisotropic and isotropic thermal parameters, free energy values, and coalescence temperatures. The complete set of data (11 pages) may be purchased from: The Depository of Unpublished Data, Document Delivery, CISTI, National Research Council of Canada, Ottawa, Canada K1A 0S2. Tables of atomic coordinates for the non-hydrogen atoms and additional bond distances and angles have also been deposited with the Cambridge Crystallographic Data Centre, and can be obtained on request from The Director, Cambridge Crystallographic Data Centre, University Chemical Laboratory, 12 Union Road, Cambridge, CB2 1EZ, U.K. Two tables of observed and calculated structure factors (94 pages) can be obtained from the corresponding author.

**Table 3.** Selected bond distances (Å) and angles (deg) for $(L\text{-}L)_2W(CO)Br_2$.

| Bond | Distance (Å) | Bond | Distance (Å) |
|---|---|---|---|
| W—As(1) | 2.573(2) | W′—As(1)′ | 2.575(2) |
| W—As(2) | 2.626(3) | W′—As(2)′ | 2.620(2) |
| W—As(3) | 2.578(3) | W′—As(3)′ | 2.577(2) |
| W—As(4) | 2.585(2) | W′—As(4)′ | 2.584(2) |
| W—Br(1) | 2.624(3) | W′—Br(1)′ | 2.624(3) |
| W—Br(2) | 2.647(3) | W—Br(2)′ | 2.664(3) |
| W—C(1) | 1.78(2) | W′—C(1)′ | 1.78(2) |
| C(1)—O(1) | 1.22(3) | C(1)′—O(1)′ | 1.19(3) |
| **Bond** | **Angle (deg)** | **Bond** | **Angle (deg)** |
| As(1)-W-As(2) | 80.30(8) | W-As(1)-C(2) | 121.0(7) |
| As(3)-W-As(4) | 75.63(8) | W-As(1)-C(3) | 116.1(8) |
| As(1)-W-Br(1) | 76.51(9) | W-As(1)-C(4) | 110.6(7) |
| As(1)-W-Br(2) | 71.9(9) | C(2)-As(1)-C(3) | 100(1) |
| As(1)-W-As(3) | 137.36(8) | C(2)-As(1)-C(4) | 100(1) |
| As(1)-W-As(4) | 145.91(9) | C(3)-As(1)-C(4) | 106(1) |
| As(1)-W-C(1) | 84.5(7) | W-As(2)-C(5) | 106.1(7) |
| As(2)-W-C(1) | 164.8(7) | W-As(2)-C(8) | 121.8(8) |
| As(2)-W-Br(1) | 82.30(10) | W-As(2)-C(9) | 118.9(7) |
| As(2)-W-Br(2) | 76.51(10) | C(5)-As(2)-C(8) | 98.7(9) |
| As(2)-W-As(3) | 106.17(9) | C(5)-As(2)-C(9) | 104(1) |
| As(2)-W-As(4) | 100.57(8) | C(8)-As(2)-C(9) | 103(1) |
| As(3)-W-Br(1) | 145.51(9) | W-As(3)-C(10) | 124.1(7) |
| As(3)-W-Br(2) | 69.00(9) | W-As(3)-C(11) | 110.8(8) |
| As(3)-W-C(1) | 85.9(7) | W-As(3)-C(12) | 113.9(7) |
| As(4)-W-C(1) | 91.2(7) | C(10)-As(3)-C(11) | 103(1) |
| As(4)-W-Br(1) | 69.93(8) | C(10)-As(3)-C(12) | 99(1) |
| As(4)-W-Br(2) | 141.77(10) | C(11)-As(3)-C(12) | 102(1) |
| Br(1)-W-C(1) | 92.9(7) | W-As(4)-C(13) | 114.4(6) |
| Br(2)-W-C(1) | 100.1(7) | W-As(4)-C(16) | 120.5(7) |
| Br(1)-W-Br(2) | 144.39(10) | W-As(4)-C(17) | 115.6(7) |
| As(3)-W-As(4) | 75.63(8) | C(13)-As(4)-C(16) | 103(1) |
| As(1)′-W′-As(2)′ | 80.38(8) | C(13)-As(4)-C(17) | 97(1) |
| As(3)′-W′-As(4)′ | 75.75(8) | C(16)-As(4)-C(17) | 102(1) |
| As(1)′-W′-Br(1)′ | 77.03(8) | W-C(1)-O(1) | 176(1) |
| As(1)′-W′-Br(2)′ | 71.72(9) | W′-As(1)′-C(2)′ | 122.2(6) |
| As(1)′-W′-As(3)′ | 136.89(8) | W′-As(1)′-C(3)′ | 116.1(7) |
| As(1)′-W′-As(4)′ | 146.41(9) | W′-As(1)′-C(4)′ | 110.0(7) |
| As(1)′-W′-C(1)′ | 85.3(7) | C(2)′-As(1)′-C(3)′ | 99(1) |
| As(2)′-W′-C(1)′ | 165.7(7) | C(2)′-As(1)′-C(4)′ | 100(1) |
| As(2)′-W′-Br(1)′ | 82.50(10) | C(3)′-As(1)′-C(4)′ | 106(1) |
| As(2)′-W′-Br(2)′ | 77.20(9) | W′-As(2)′-C(5)′ | 106.9(7) |
| As(2)′-W′-As(3)′ | 105.95(9) | W′-As(2)′-C(8)′ | 121.3(7) |
| As(2)′-W′-As(4)′ | 100.07(8) | W′-As(2)′-C(9)′ | 119.1(7) |
| As(3)′-W′-Br(1)′ | 145.50(9) | C(5)′-As(2)′-C(8)′ | 99(1) |
| As(3)′-W′-Br(2)′ | 68.53(8) | C(5)′-As(2)′-C(9)′ | 103(1) |
| As(3)′-W′-C(1)′ | 84.9(7) | C(8)′-As(2)′-C(9)′ | 103(1) |
| As(4)′-W′-C(1)′ | 91.5(6) | W′-As(3)′-C(10)′ | 123.9(7) |
| As(4)′-W′-Br(1)′ | 69.81(8) | W′-As(3)′-C(11)′ | 110.8(7) |
| As(4)′-W′-Br(2)′ | 141.55(10) | W′-As(3)′-C(12)′ | 113.7(7) |
| Br(1)′-W′-C(1)′ | 93.8(7) | C(10)′-As(3)′-C(11)′ | 104(1) |
| Br(2)′-W′-C(1)′ | 98.9(6) | C(10)′-As(3)′-C(12)′ | 99(1) |
| Br(1)′-W′-Br(2)′ | 145.00(10) | C(11)′-As(3)′-C(12)′ | 102(1) |
| As(3)′-W′-As(4)′ | 75.75(8) | W′-As(4)′-C(13)′ | 114.9(7) |
| W′-As(4)′-C(16)′ | 120.0(7) | C(13)′-As(4)′-C(17)′ | 99(1) |
| W′-As(4)′-C(17)′ | 114.4(7) | C(16)′-As(4)′-C(17)′ | 102(1) |
| C(13)′-As(4)′-C(16)′ | 103(1) | W′-C(1)′-O(1)′ | 175(1) |

**Fig. 2.** Schematic diagram showing the torsional angles in the five-membered ring of the chelate ligand for $(L\text{-}L)W(CO)_2I_2P(OC_6H_5)_3$ (top numbers) and the related complex $(L\text{-}L)W(CO)_2I_2P(OCH_3)_3$ (bottom numbers).

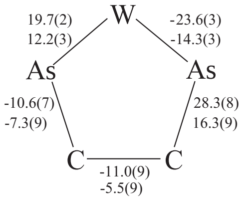

mixture at –20°C under an inert atmosphere. A hexagonal plate with approximate dimensions 0.39 × 0.22 × 0.19 mm was selected and coated with collodion. Precession photographs showed systematic extinction conditions ($h0l$: $l = 2n$; $0k0$: $k = 2n$) and symmetry indicative of the space group $P2_1/c$. The accurate unit cell parameters were obtained from the least-squares refinement of 36 reflections in the 2θ range 25–45°, observed as for the previous compound. The data were collected at 203 ± 4 K. The intensities of three standard reflections, measured after every 47 data points, showed an average decay of 20% over the period of the data collection.

The intensities of 7611 reflections were measured ($hkl$, $hk\bar{l}$ for 2θ values in the range 3–45°) of which 5364 were considered to be observed with $I \geq 2\sigma(I)$. The data were corrected for the decay in the standard reflections, and absorption corrections were applied as for the previous compound. Faces of the crystal were not well defined and were approximated. The crystal data are given in Table 1. The structure has two independent molecules in the unit cell. The structure was solved by the heavy-atom method, using direct methods to confirm the positions of the two tungsten atoms. The remaining non-hydrogen atoms were found from successive Fourier maps. The positions of the hydrogen atoms were not apparent on the difference maps. The structure was refined by full-matrix least squares, treating the tungsten, arsenic, bromine, and fluorine atoms anisotropically and the carbon and oxygen atoms isotropically. Weights were assigned as $w = \sigma_c^{-2}$, where $\sigma_c^2$ is the variance in $F$ as calculated from counting statistics and the instability factor.

The refinement converged to a conventional $R$ value of 0.073 and a weighted $R$ value of 0.10. These high values reflect the decay of the sample during data collection and the poor quality of the sample as manifested by a large number of weak reflections. The maximum and average shift/esd were $1.2 \times 10^{-3}$ and $3.1 \times 10^{-5}$, respectively, at the end of refinement. The coordinates of the two independent molecules were approximately related by the operator $1/2 + x$, $1/2 - y$, $z$. If this relation were exact, reflections $h0l$ would be absent. The data showed that these reflections were weak but not absent. Further examination showed that they were not due to multiple scattering. Therefore, the apparent symmetry is only approximate. Pairs of residual electron-density peaks, with a maximum height of 3.6 e Å$^{-3}$, were observed near each of the tungsten, bromine, and arsenic atoms, reflecting the limitations in the approximate absorption corrections.

All calculations were carried out using the XTAL 2.4 system of programs (22). Important bond lengths and angles are given in Table 3. The labelling for the two molecules are

**Fig. 3.** ORTEP diagram for (L-L)$_2$W(CO)Br$_2$ showing the atomic labelling scheme for the unprimed molecule with 50% probability thermal ellipsoids.

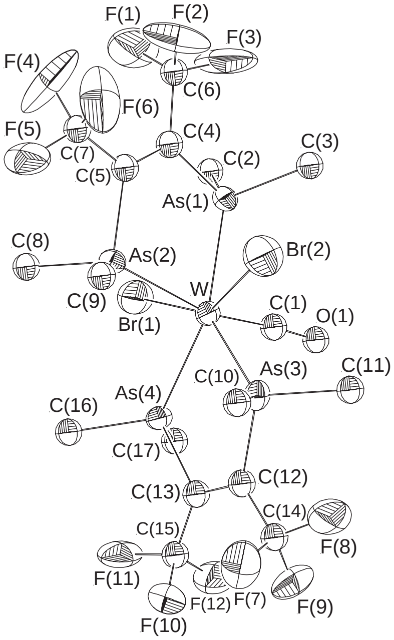

identical except that the chemical symbols for one are primed. An ORTEP drawing showing the labelling scheme for the unprimed molecule is given in Fig. 3.

## Results and discussion

### Synthesis of the seven-coordinate complexes

The dicarbonyl complexes containing a monodentate phosphine or phosphite ligand were readily synthesized from the corresponding tricarbonyl complexes in refluxing benzene. More vigorous conditions (refluxing toluene) were necessary to form the monocarbonyl complexes; attempts yielded only (L-L)$_2$W(CO)X$_2$ and (L-L)W(CO)X$_2$[P(OCH$_3$)$_3$]$_2$ (X = Br, I). Presumably there is congestion around the tungsten atom with ligands such as P(C$_6$H$_5$)$_3$, P(OC$_6$H$_5$)$_3$, P(OC$_2$H$_5$)$_3$, and P(C$_4$H$_9$)$_3$.

### Crystal structure of (L-L)W(CO)$_2$I$_2$P(OC$_6$H$_5$)$_3$

The tungsten atom is seven-coordinate with the coordination sphere containing the two arsenic atoms of the L-L ligand, two iodine atoms, two carbon atoms of the carbonyl groups, and the phosphorus atom of the triphenylphosphite group. To determine the stereochemistry of the title compound we have used the δ parameters of Porai–Koshits and Aslanov (23), as calculated by Muetterties and Guggenberger (13). The δ parameter values (21°, 17°, 6°), when compared with the idealized monocapped octahedron (24.2°, 24.2°, 24.2°) and the idealized monocapped trigonal prism (0°, 0°, 41.5°), indicate the geometry to be closer to a monocapped octahedron. For this geometry the capping atom is the C(2) carbonyl group with the capped face containing the As(1), C(1), and P atoms. Kepert (24) has shown that seven-coordinate complexes containing one bidentate ligand with a normalized *bite* (defined as the distance between points representing the donor atoms of the bidentate ligands on a sphere of unit radius and with the same angles subtended at the center as in the real coordination polyhedron) less than 1.11 would be expected to exhibit pentagonal–bipyramidal geometry, and those with a normalized *bite* greater than 1.11 would be expected to exhibit either monocapped octahedral or monocapped trigonal prismatic geometry. The observed geometry of the tungsten complex with a normalized *bite* of 1.24 for the L-L ligand is in accord with Kepert's (24) conclusions. A similar geometry is observed for the related complex (L-L)W(CO)$_2$I$_2$P(OCH$_3$)$_3$ with an L-L normalized *bite* of 1.23 (11). Both complexes also exhibit other features associated with a monocapped octahedral geometry. The mean C$_c$-W-A$_c$ and C$_c$-W-A$_u$ angles (C$_c$ is a capping atom, A$_c$ is an atom in the capped face, and A$_u$ is an atom in the uncapped face) are 73.4° and 127.3° for the triphenylphosphite compound and 72.7° and 127.8° for the trimethyl phosphite complex (11), respectively, with corresponding angles for an ideal monocapped octahedron being 74.1° and 125.5° (25). The other feature is that the unique capping atom has very close contacts with the three atoms in the capped face. Thus in the triphenylphosphite complex the capping carbon is 2.27, 2.69, and 2.77 Å from the C, As, and P atoms, respectively, in the capped face and in the related trimethyl phosphite complex 2.28, 2.71, and 2.69 Å from these atoms (11).

The five-membered ring of the chelate ligand shows a moderate degree of puckering in both the triphenylphosphite and trimethyl phosphite complexes. The torsional angles for both complexes are shown in Fig. 2. The ring-puckering parameters, according to the method of Cremer and Pople (26) are $q = 0.42$ and $\phi = 14°$ for (L-L)W(CO)$_2$I$_2$P(OC$_6$H$_5$)$_3$ and $q = 0.26$ and $\phi = 10.1°$ for (L-L)W(CO)$_2$I$_2$P(OCH$_3$)$_3$ (11), indicating a moderate degree of puckering, intermediate between a twist and envelope conformation. The greater degree of puckering in the triphenylphosphite complex is primarily due to the presence of the bulky phenyl rings compared to the methyl groups. The tetrahedral coordination of the arsenic atoms is also distorted by the contacts.

The two carbon monoxide ligands are in a *cis* arrangement to each other (71.2°), the arrangement required in order to minimize competition for dπ electron density from the d$^4$ tungsten atom. The lengths of the two W—As bonds are significantly different from each other at 2.5603(7) and 2.6004(7) Å, which can be explained by a consideration of their respective *trans* ligands. The I(1) atom *trans* to As(1) is not as strong an acceptor as the P atom *trans* to As(2), resulting in greater back donation to As(1). This results in a shortening of the W—As(1) bond compared to the W—As(2) bond, the difference being 0.04(1) Å. The average W—I bond length of 2.87 Å in this complex is close to the average of 2.85 Å reported for similar complexes (27, 28). The W—P bond length of 2.457(2) Å is similar to that in (L-L)W(CO)$_2$I$_2$P(OCH$_3$)$_2$ (2.466(3) Å) (11) but considerably shorter as compared to (L-L)W(CO)$_2$Br$_2$P(C$_6$H$_5$)$_3$ (2.548(2) Å) (12). This difference may reflect both the steric restrictions of the greater bulk of the P(C$_6$H$_5$)$_3$ groups and the presence of more double-bond character through back donation from the tungsten in (L-L)W(CO)$_2$I$_2$P(OC$_6$H$_5$)$_3$. These results are in accord with differences in the π-acceptor ability of the phosphorus ligands.

### Crystal structure of (L-L)$_2$W(CO)Br$_2$

The structure contains two crystallographically independent

**Fig. 4.** Schematic diagram showing the torsional angles in the two five-membered rings of the chelate ligands for $(L\text{-}L)_2W(CO)Br_2$. As(1) and As(2) occupy equatorial and axial positions, respectively; As(3) and As(4), equatorial positions. The top numbers refer to each ring of the unprimed molecule and the bottom numbers to each corresponding ring of the primed molecule.

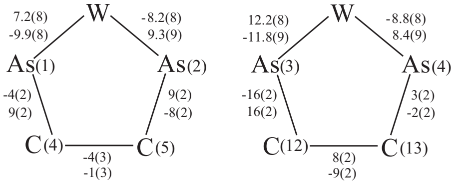

**Table 4.** The ν(CO) and $^{13}C$ NMR data (carbonyl region) for seven-coordinate complexes.

| Complex | ν(CO) (cm$^{-1}$)$^a$ | δ (ppm)$^b$ | $^2J(^{13}C\text{-}^{31}P)$ (Hz) |
|---|---|---|---|
| $(L\text{-}L)W(CO)_2I_2P(OC_6H_5)_3$ | 1959 (vs) | 212.4(d) | 9.3 |
| | 1875 (s) | 240.4(d) | 39.9 |
| $(L\text{-}L)W(CO)_2Br_2P(OC_6H_5)_3$ | 1956 (vs) | 217.0(d) | 8.3 |
| | 1872 (s) | 245.8(d) | 37.0 |
| $(L\text{-}L)W(CO)_2I_2P(OCH_3)_3$ | 1948 (vs) | 215.0(d) | 9.7 |
| | 1870 (s) | 240.4(d) | 42.1 |
| $(L\text{-}L)W(CO)_2Br_2P(OCH_3)_3$ | 1950 (vs) | 220.0(d) | 5.8 |
| | 1868 (s) | 246.1(d) | 39.6 |
| $(L\text{-}L)W(CO)_2I_2P(C_6H_5)_3$ | 1937 (vs) | 216.7(d) | 5.1 |
| | 1855 (s) | 246.5(d) | 29.0 |
| $(L\text{-}L)W(CO)_2Br_2P(C_6H_5)_3$ | 1940 (vs) | 222.2(d) | 5.0 |
| | 1854 (s) | 250.8(d) | 27.3 |
| $(L\text{-}L)W(CO)I_2[P(OCH_3)_3]_2$ | 1833 | 254.8(dd) | 37.0, 39.6 |
| $(L\text{-}L)W(CO)Br_2[P(OCH_3)_3]_2$ | 1829 | 259.0(dd) | 34.8, 36.0 |
| $(L\text{-}L)_2W(CO)I_2$ | 1811 | 241.5(s) | |
| $(L\text{-}L)_2W(CO)Br_2$ | 1809 | 260.5(s) | |

[a] Spectra were recorded in $CH_2Cl_2$; vs = very strong, s = strong.

[b] Spectra were recorded in $CD_2Cl_2$ at 200 K in the presence of a trace amount of $[Cr(acac)_3]$; s = singlet, d = doublet, dd = doublet of doublets.

molecules that are related as near enantiomers. They are chemically equivalent; equivalent metal—ligand bond distances differ by less than 0.02 Å, equivalent interligand distances differ by an average of 0.04 Å, and intramolecular bond angles agree within 2.5°. In both molecules the two L-L ligands chelate the metal to form a seven-coordinate tungsten (II) complex with the two bromine atoms and the carbonyl group. The tungsten atom has a slightly distorted pentagonal bipyramidal geometry. The δ parameters of Porai–Koshits and Aslanov (23) are 37° and 52°. In the pentagonal bipyramid the third δ parameter represents an interatomic vector internal to the polyhedron. The δ values for an ideal pentagonal bipyramid with identical ligands are both 54.4°. The equatorial plane of the pyramid is occupied by an L-L ligand, the two bromine atoms, and one arsenic atom of the other L-L ligand, leaving the second arsenic atom and the carbonyl group to fill the apical positions. The tungsten atom is displaced from the average plane of the pentagonal ring by 0.0144(2) Å. Thus this less symmetric pentagonal bipyramid has fewer steric constraints than the more symmetric one with both L-L ligands in the pentagonal plane, with repulsions between the methyl groups on adjacent arsenic atoms.

This type of geometry is rare (29, 30) for seven-coordinate carbonyl complexes of the type $MX_2(CO)_nL_{5-n}$ (M = Mo, W; $n$ = 1–3). The tungsten—carbon bond is unique, being extremely short (1.78(2) Å) compared to a related monocarbonyl complex (10) containing two monodentate $P(OCH_3)_3$ ligands (1.86(3) Å) and the related dicarbonyl complexes (11, 12) (average 1.94 Å). The relative shortness of the tungsten—carbon bond here represents considerable double-bond character arising from back donation of π electrons from tungsten.

The four five-membered rings of the chelate ligands in the two independent molecules of $(L\text{-}L)_2W(CO)Br_2$ show a variation in conformation. Their torsional angles are shown in Fig. 4. One of the two chelates in each independent molecule has a *bite* that spans from the equatorial plane of the pentagonal bipyramid to one of the axial vertices (equatorial–axial), involving the atoms As(1) and As(2). The other chelate in each molecule has a *bite* that forms an edge of the equatorial plane (equatorial–equatorial), involving the atoms As(3) and As(4).

Because of the approximate enantiomorphic relation between the two independent molecules, the torsional angles of their equatorial–equatorial five-membered rings have similar torsional angle magnitudes but with opposite signs. This is further illustrated by the ring-puckering parameters of Cremer and Pople (26), which show similar puckering amplitudes (0.20 for each) and puckering phase angles different by approximately 180° (200° in one molecule and 22° in the other molecule). These phase angles correspond to the twist conformation of a five-membered ring. The equatorial–axial chelates are less similar, with puckering amplitudes of 0.15 and 0.18, and the respective puckering phase angles of 168° and 1°. These phase angles correspond to an intermediate twist-boat conformation and a boat conformation, respectively. In this case, four of the torsional angles show opposite signs, with the fifth small and negative in both cases.

## Spectroscopic properties of $(L\text{-}L)W(CO)_2I_2P(OC_6H_5)_3$ and related seven-coordinate dicarbonyl complexes

Table 4 lists carbonyl IR stretching frequencies and $^{13}C$ NMR data, and Table 5 lists $^{19}F\text{-}\{^1H\}$and $^{31}P\text{-}\{^1H\}$NMR data for all the seven-coordinate complexes under study. The observation of a single $As\text{–}CH_3$ resonance in the $^1H$ NMR spectrum (297 K) and a single $CF_3$ resonance in the $^{19}F\text{-}\{^1H\}$NMR spectrum of $(L\text{-}L)W(CO)_2I_2P(OC_6H_5)_3$ are not consistent with the molecule having a static solution structure equivalent to that determined from the X-ray determination. The static structure consistent with the solid-state structure is frozen out at 200 K. Thus, $As\text{–}CH_3$ resonances are found at 1.50, 1.84, 2.51, two $CF_3$ quartets at –52.2 and –53.8, and two $^{13}C$ doublets (carbonyl region) at 212.4 and 240.4. It is assumed that accidental degeneracy may have caused the 1:2:1 $As\text{–}CH_3$ triplet, since all other related complexes exhibited four equal-area $As\text{–}CH_3$ resonances. The dicarbonyl complexes are related as shown by the similarity of carbonyl stretching frequencies, chemical shifts, coupling constants, and variable temperature $^1H$ and $^{19}F\text{-}\{^1H\}$NMR data. As the temperature is increased, four $As\text{–}CH_3$ peaks (three for the title compound) indicative of the low-temperature slow-exchange limiting spectra coalesce into two peaks. The line broadening continues until an averaged

**Table 5.** The $^{19}F$-{$^{1}H$} and $^{31}P$-{$^{1}H$} NMR data for seven-coordinate complexes.

| Complex | δ($^{19}F$) (ppm)$^{a}$ | | $J(^{19}F\text{-}^{19}F)$ (Hz) | δ($^{31}P$) (ppm)$^{b}$ | $J(^{31}P\text{-}^{183}W)$ (Hz) |
|---|---|---|---|---|---|
| | 297 K | 210 K | | | |
| (L-L)W(CO)$_2$I$_2$P(OC$_6$H$_5$)$_3$ | –53.1 (s) | –52.2 (q, 3F) | 14.3 | 90.7 | 402.8 |
| | | –53.8 (q, 3F) | | | |
| (L-L)W(CO)$_2$Br$_2$P(OC$_6$H$_5$)$_3$ | –51.4 (s) | –50.7 (q, 3F) | 14.1 | 101.1 | 406.1 |
| | | –52.3 (q, 3F) | | | |
| (L-L)W(CO)$_2$I$_2$P(OCH$_3$)$_3$ | –51.5 (s) | –51.5 (m, 6F) | — | 104.7 | 364.7 |
| (L-L)W(CO)$_2$Br$_2$P(OCH$_3$)$_3$ | –51.3 (s) | –51.4 (m, 6F) | — | 112.3 | 377.1 |
| (L-L)W(CO)$_2$I$_2$P(C$_6$H$_5$)$_3$ | –52.2 (s) | –52.3 (m, 6F) | — | –7.1 | 216.1 |
| (L-L)W(CO)$_2$Br$_2$P(C$_6$H$_5$)$_3$ | –51.1 (s) | –51.4 (m, 6F) | — | 4.8 | 222.3 |
| (L-L)W(CO)I$_2$[P(OCH$_3$)$_3$]$_2$ | –52.7 (s) | –53.0 (q, 3F) | 14.3 | 104.5 | 411.9 |
| | | –54.1 (q, 3F) | | 130.2 | 389.5 |
| | | | | $^{2}J(^{31}P\text{-}^{31}P) = 31.9$ Hz | |
| (L-L)W(CO)Br$_2$[P(OCH$_3$)$_3$]$_2$ | –51.7 (s) | –51.1 (q, 3F) | 14.3 | 113.5 | 418.1 |
| | | –52.3 (q, 3F) | | 138.3 | 384.5 |
| | | | | $^{2}J(^{31}P\text{-}^{31}P) = 30.8$ Hz | |
| (L-L)$_2$W(CO)I$_2$ | –50.7 (s) | –51.0 (m) | — | — | — |
| (L-L)$_2$W(CO)Br$_2$ | –50.6 (s) | –51.0 (m) | — | — | — |

[a] Spectra were recorded in CD$_2$Cl$_2$; s = singlet, q = quartet, m = A$_3$B$_3$ multiplet.

[b] Each resonance (297 K) appeared as a singlet with $^{183}W$ satellites except for (L-L)W(CO)X$_2$[P(OCH$_3$)$_3$]$_2$ (X = Br, I) for which each resonance (210 K) appeared as a doublet with $^{183}W$ satellites.

single As–CH$_3$ resonance is observed, indicative of the high-temperature fast-exchange limiting spectra.

The $^{13}C$ chemical shifts (carbonyl region), carbonyl stretching frequencies, and $J(^{31}P\text{-}^{183}W)$ values are consistent with the electronic differences of the three phosphorus monodentate ligands in which P(C$_6$H$_5$)$_3$ is a better net donor: P(OC$_6$H$_5$)$_3$, P(OCH$_3$)$_3$, P(C$_6$H$_5$)$_3$. An examination of the low-temperature $^{13}C$ chemical shifts in Table 4 shows two unique resonances for the dicarbonyl complexes, one that is approximately 30 ppm downfield from the other. For the title dicarbonyl complex the downfield resonance is assigned to the unique capping carbonyl group consistent with the work of Colton and Kevekordes (31), where they assigned the low field carbonyl chemical shift absorption to the capping carbon in a structure best described as a monocapped octahedron. Another unique feature of the $^{13}C$ NMR data is the large differences in $^{2}J(^{13}C\text{-}^{31}P)$ values that are consistent with *cis* coupling. Previous work has shown an average $^{2}J(^{13}C\text{-}^{31}P)$ value of 32 Hz for angles subtended at tungsten by the phosphorus and carbonyl carbon in the range of 72–78° and a $^{2}J(^{13}C\text{-}^{31}P)$ value of 6 Hz for a corresponding angle of 95° (25, 32–34). On this basis the larger $^{2}J(^{13}C\text{-}^{31}P)$ value could be assigned to the carbonyl with a P-W-C angle in the range 70–80° and the lower $^{2}J(^{13}C\text{-}^{31}P)$ value to the carbonyl with a P-W-C angle above 100°. For the title dicarbonyl complex, the capping carbonyl (<P-W-C = 77.2°) is assigned the resonance with $^{2}J(^{13}C\text{-}^{31}P) = 39.9$ Hz, and the noncapping carbonyl (<P-W-C = 110.7°) the resonance with $^{2}J(^{13}C\text{-}^{31}P) = 9.3$ Hz. These assignments are compatible with the earlier assignments made for the carbonyl group chemical shift on the basis of the unique capping position.

In view of the difficulty in assigning a configuration for seven-coordinate complexes based on multinuclear NMR data, we believe $^{13}C$ chemical shifts and $^{2}J(^{13}C\text{-}^{31}P)$ values provide important insights in elucidating structural considerations.

There have been many possible pathways suggested to explain the fluxional behaviour in seven-coordinate compounds involving dissociative processes and intramolecular rearrangements. Dissociative processes such as phosphite or phosphine dissociation or carbonyl dissociation for the dicarbonyl complexes can be eliminated by the fact that the $^{31}P$-{$^{1}H$}fast-exchange limiting NMR spectra exhibited $^{31}P\text{-}^{183}W$ coupling, and $^{13}C$ fast-exchange limiting NMR spectra exhibited both $^{13}C\text{-}^{183}W$ and $^{13}C\text{-}^{31}P$ coupling. Dissociation of one end of the chelated ligand would probably require a much higher barrier than that which is observed ($\Delta G^{\neq}$ values in the range 45.1–54.0 kJ/mol).

The activation energy barriers $\Delta G^{\neq}$ for methyl group exchange (calculated from the Eyring equation (35) at the coalescence temperature) show an increase, with an increase in the size of the halide and the bulk of the phosphorus ligand, consistent with an intramolecular process (36) in which the tungsten—halide and tungsten—phosphorus bonds are retained throughout the dynamic process.

To explain the dynamic behaviour of the title compound an exchange process can be envisaged, which itself varies over a narrow temperature range. The process might begin with random scrambling of the atoms I(1), C(1), and P, leaving the atom I(2) rigidly held in the "pocket" of the chelate ring. This would equilibrate the atoms C(4) and C(9) as one pair, and the atoms C(3) and C(10) as the other pair. As the temperature is raised further the atom I(2) is gradually added to the random scrambling motion, causing coalescence to a single peak. The $\Delta G^{\neq}$ value associated with the lower temperature part of the process is 51.7(2) kJ/mol and with the higher temperature part of the process is 54.0(2) kJ/mol. The similarity of these two values supports the description of the phenomenon responsible for the coalescence as being one process.

## Spectroscopic properties of (L-L)$_2$W(CO)Br$_2$ and related seven-coordinate monocarbonyl complexes

As with the previous complex, the observations of a single As–CH$_3$ resonance in the $^{1}H$ NMR spectrum (297 K) and a

**Fig. 5.** Schematic diagram illustrating a pathway for the dynamic behaviour for (L-L)$_2$W(CO)Br$_2$.

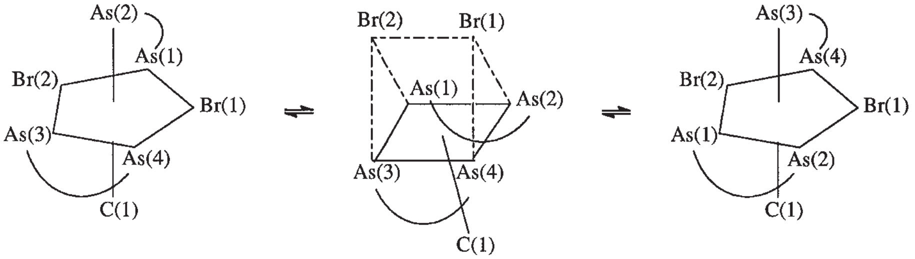

**Fig. 6.** Schematic diagram illustrating a pathway for the dynamic behaviour for (L-L)W(CO)Br$_2$[P(OCH$_3$)$_3$]$_2$.

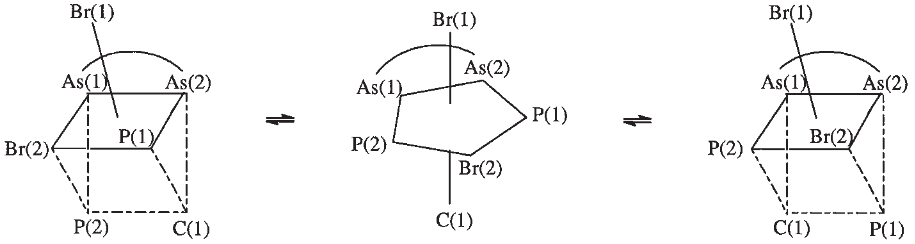

single CF$_3$ resonance in the $^{19}$F-{$^1$H}NMR spectrum of (L-L)$_2$W(CO)Br$_2$ are not consistent with the X-ray crystal structure, suggesting dynamic behaviour. Lowering the temperature to 180 K produced two As–CH$_3$ resonances at 1.76 and 2.15 and a complex CF$_3$ multiplet centred at –51.0. Further lowering of the temperature to 170 K (lowest attainable due to solvent limitations) caused the low field As–CH$_3$ resonance to broaden. Thus it was not possible to obtain a low-temperature slow-exchange limiting spectrum indicative of the solid-state X-ray crystal structure. The $\Delta G^{\neq}$ value of 43.5 kJ/mol is comparatively low for a complex containing two bidentate ligands relative to the dicarbonyl complexes; perhaps the small *bite* of the two L-L ligands provides extra space around the tungsten centre for other ligands, thus enhancing the possibility for rearrangements.

A nondissociative mechanism consistent with the NMR data could involve a concerted rearrangement in which the roles of the two bidentate L-L ligands are reversed, and the environments of their methyl groups are also equilibrated. An intermediate polyhedron between the two pentagonal bipyramidal geometries is a monocapped trigonal prism, with the carbonyl ligand capping the quadrilateral face formed by the four arsenic atoms as illustrated in Fig. 5. Then the polyhedron found in the crystal can be generated from it by moving any one of the four As atoms through the Br- -Br edge of that polyhedron to become the apical polyhedron of the pentagonal bipyramid, leaving its ligand mate near the pentagonal plane between the two Br atoms.

If the pentagonal symmetry is not fully formed, as is seen in the crystal structure, then there will be a tendency for relaxation back to the monocapped trigonal prism intermediate polyhedron to proceed along the same route as that by which the pentagonal bipyramid was formed. This would then leave two broad peaks, corresponding to the As–CH$_3$ resonances for the CH$_3$ on the two sides of the plane of the intermediate. The deviations from the full symmetry of the pentagonal bipyramid are associated with the puckering of the plane of the bidentate ligand. However, if the full symmetry of the pentagonal bipyramid is formed at higher temperature, then relaxation back to the intermediate polyhedron may take place with equal probability for the apical As to arrive back in the monocapped trigonal pyramid sharing an edge with Br(1) or with Br(2). Then all eight As–CH$_3$ resonances would be equilibrated.

Attempts to produce other related monocarbonyl complexes have only yielded (L-L)W(CO)X$_2$[P(OCH$_3$)$_3$]$_2$ (X = Br, I). We have previously published the X-ray crystal structure of (L-L)W(CO)Br$_2$[P(OCH$_3$)$_3$]$_2$ (10) and have included extensive spectroscopic data in the present paper. Low-temperature NMR studies of the trimethylphosphite monocarbonyl complex suggest a static structure consistent with the X-ray crystal structure (best described as a monocapped trigonal prism with a Br in the capping position and two As atoms, a P, and a Br atom in the quadrilateral capped face; four $^1$H As-CH$_3$ singlets; and two $^{31}$P-{$^1$H}doublets). As the temperature is increased the four As–CH$_3$ resonances coalesce into two and then into an averaged As–CH$_3$ resonance. Similarly, the two $^{31}$P-{$^1$H}doublets coalesce into a single resonance with $^{183}$W satellites. The $\Delta G^{\neq}$ values (51.3 and 69.7 kJ/mol) are considerably higher than the previously discussed monocarbonyl containing the two bidentate L-L ligands, reflecting a greater steric hindrance exerted by the bulkier P(OCH$_3$)$_3$ monodentate ligands. The equilibration of four As–CH$_3$ resonances into two and two $^{31}$P resonances into one can be rationalized by the dynamic behaviour illustrated in Fig. 6, producing a pentagonal bipyramidal intermediate with As$_1$As$_2$Br$_2$P$_1$P$_2$ in the equatorial plane. This would equilibrate the As–CH$_3$ groups above the pentagonal plane as one set and As–CH$_3$ groups below the pentagonal plane as the other set as well as equilibrating the two $^{31}$P environments of the trimethylphosphite ligands. The equilibration of two As–CH$_3$ resonances into one at a coalescence temperature of 348 K occurs with a higher activation energy than that for the first process (69.7 vs. 51.3 kJ/mol), suggesting either a dissociative process or a high-energy random scrambling process. The possibility of phosphorus dissociation can be eliminated on the basis of the retention of $J$($^{31}$P-$^{183}$W) coupling in the high-temperature fast-exchange limiting spectra.

Finally, the low-temperature $^{13}$C NMR data (carbonyl region) are consistent with *cis* coupling on the basis of $^2J(^{13}C-^{31}P)$ values (Table 4), and the values of 34.8 and 36.0 Hz for the bromomonocarbonyl are consistent with the angles subtended at tungsten by the phosphorus and carbonyl carbon atoms (71° and 76°) (10), a correlation previously discussed for the dicarbonyl complexes.

To determine the influence of the bidentate ligand and to provide additional $^{31}P$ NMR parameters that were lacking in this study further work is continuing in the area of seven coordination incorporating the ligands $(C_6H_5)_2PCH_2P(C_6H_5)_2$, $(C_6H_5)_2PCH_2CH_2P(C_6H_5)_2$, and *cis*-$(C_6H_5)_2PCH{=}CHP(C_6H_5)_2$. This work is aimed at the study of monocarbonyl complexes containing two identical bidentate ligands and two different bidentate ligands. In addition the potential use of $^{183}W$ NMR is being investigated.

## Acknowledgment

We thank the Faculty of Science, University of Regina, for financial support and Quinn Major for computing assistance.

## References

1. F.A. Cotton, L.R. Falvello, and J.H. Meadows. Inorg. Chem. **24**, 514 (1985).
2. A. Mercer and J. Trotter. Can. J. Chem. **52**, 3331 (1974).
3. A.L. Beauchamp, F. Belanger-Gariepy, and S. Arali. Inorg. Chem. **24**, 1860 (1985).
4. M.G.B. Drew and J.D. Wilkins. J. Chem. Soc. Dalton Trans. 2664 (1973).
5. F.A. Cotton and M. Matusz. Polyhedron, **6**, 261 (1987).
6. A. Blagg, A.T. Hutton, and B.L. Shaw. Polyhedron, **6**, 95 (1987).
7. P.K. Baker, M.B. Hursthouse, A.I. Karaulov, A.J. Lavery, K.M. Abdul Malik, D.J. Muldoon, and A. Shawcross. J. Chem. Soc. Dalton Trans. 3493 (1994).
8. R.P.K. Babu, S.S. Krishnamurthy, and M. Nethaji. Organometallics, **14**, 2047 (1995).
9. P.K. Baker, M.E. Harman, S. Hughes, M.B. Hursthouse, and K.M. Abdul Malik. J.Organomet. Chem. **498**, 257 (1995).
10. L. Mihichuk, M. Pizzey, B. Robertson, and R. Barton. Can. J. Chem. **64**, 991 (1986).
11. L.M. Mihichuk, C.L. Giesinger, B.E. Roberston, and R.J. Barton. Can. J. Chem. **65**, 2634 (1987).
12. S.K. Manocha, L.M. Mihichuk, R.J. Barton, and B.E. Robertson. Acta Crystallogr. Sect. C, **C47**, 722 (1991).
13. E.L. Muetterties and L.J. Guggenberger. J. Am. Chem. Soc. **96**, 1748 (1974).
14. M.G.B. Drew. Prog. Inorg. Chem. **23**, 67 (1977).
15. M.G.B. Drew and C.J. Rix. J. Organomet. Chem. **102**, 467 (1975).
16. W.R. Cullen and L.M. Mihichuk. Can. J. Chem. **54**, 2548 (1976).
17. J.L. Templeton and B.C. Ward. J. Am. Chem. Soc. **103**, 3743 (1981).
18. P.J. Domaille and S.S. Wreford. Inorg. Chem. **19**, 2188 (1980).
19. W.R. Cullen and L.M. Mihichuk. Can. J. Chem. **53**, 3401 (1975).
20. J.P. Crow, W.R. Cullen, F.G. Herring, J.R. Sams, and R.L. Tapping. Inorg. Chem. **10**, 1616 (1971).
21. H. Wang and B.E. Robertson. Structure and statistics in crystallography. Adenine Press, Giilderland, N.Y. 1985.
22. S.R. Hall and J.M. Stewart. Xtal 2.4 users manual. Universities of Western Australia and Maryland. 1988.
23. M.A. Porai-Koshits and L.A. Aslanov. Zh. Strukt. Khim. **13**, 266 (1972).
24. D.L. Kepert. Inorganic stereochemistry. Inorganic chemistry concepts. Vol. 6. Springer-Verlag, New York. 1982.
25. R.O. Day, W.H. Batschelet, and R.A. Archer. Inorg. Chem. **19**, 2113 (1980).
26. D. Cremer and J.A. Pople. J. Am. Chem. Soc. **97**, 1354 (1975).
27. M.G.B. Drew and J.D. Wilkins. J. Chem. Soc. Dalton Trans. 1654 (1974).
28. M.G.B. Drew and J.D. Wilkins. J. Organomet. Chem. **69**, 271 (1974).
29. F.A. Cotton and R. Poli. Inorg. Chem. **25**, 3703 (1986).
30. F.A. Cotton, L.R. Falvello, and R. Poli. Polyhedron, **6**, 1135 (1987).
31. R. Colton and J. Kevekordes. Aust. J. Chem. **35**, 895 (1982).
32. R.S. Herrick and J.L. Templeton. Inorg. Chem. **25**, 1270 (1986).
33. L.S. Van Der Sluys, K.A. Kubat-Martin, G.J. Kubas, and K.G. Caulton. Inorg. Chem. **30**, 306 (1991).
34. L.H. Randall, A.A. Cherkas, and A.J. Carty. Organometallics, **8**, 568 (1989).
35. J. Sandstrom. Dynamic NMR spectroscopy. Academic Press, New York. 1982.
36. L.D. Brown, S. Datta, J.K. Kouba, L.K. Smith, and S.S. Wreford. Inorg. Chem. **17**, 729 (1978), and refs. therein.